12th International Conference on Fracture Mechanics of Concrete and Concrete Structures
FraMCoS-12
B.L.A. Pichler, Ch. Hellmich, P. Preinstorfer (Eds)

https://doi.org/10.21012/FC12.1126
MS01-3:1

IMPLEMENTATION OF THE COHESIVE CRACK MODEL WITH THE FINITE PARTICLE METHOD FOR FAILURE ANALYSIS OF REINFORCED CONCRETE BEAMS

YING YU[*],HONGJIE CHEN[*],FEDERICO ACCORNERO[*],ALBERTO CARPINTERI[*]

[*] Shantou University, Department of Civil Engineering and Smart Cities
Daxue Road, 515063 Shantou, China
e-mail: 21hjchen1@stu.edu.cn, www.stu.edu.cn

Key words: Cohesive/Overlapping Crack Model(COCM),Finite Particle Method (FPM),Reinforced Concrete (RC),Size-scale effects,Failure-mode transitions

Abstract: This study presents the implementation of a Cohesive/Overlapping Crack Model (COCM) integrated with the Finite Particle Method (FPM), a meshless numerical analysis technique grounded in vector mechanics. The FPM is widely acknowledged for its efficacy in addressing dynamic, nonlinear, and fracture-related challenges. The proposed combined model provides a robust framework for accurately capturing both tensile and compressive failure mechanisms in materials, including plain and reinforced concrete. To validate the model's capability, simulations of three-point bending specimens were conducted, demonstrating its effectiveness in representing the intricate fracture behavior of concrete structures.

1 INTRODUCTION

The common way to deal with the crack problem is to adopt the embedded discontinuous model [1] and node force release method [2]. The introduction of those methods allows the FEM tosolve the discontinuous problems while is still difficult to simulate the complex crack propagation. The boundary element method and element free Galerkin method have also widely adopted for discontinuous problem [3]. However, boundary element method is difficult to deal with nonlinear problems and element free Galerkin method is hard to deal with boundary condition. Some of the most developments in FEM modelling of crack propagation are based on the partition of unity.

In this study, a new strategy based on the finite particle method is proposed to deal with the crack extension problem. Section 2 introduces the basic concepts of FPM and describes cracking in the framework of FPM. Section 3 details the proposed COCM [4] for simulating elastic cracking and FPM-COCM method, which combines the FPM and COCM for simulating crack extension in concrete beams.

2 DESCRIPTION OF CRACK PROPAGATION OF FPM

The FPM method is a vector mechanics based computation method for solid media with large rotation and large deformation, and incorporates three fundamental concepts: point value description, path element, and fictitious reverse motion.

2.1 Motion Equation

Structure deformation and rigid motion are described by particle motion, namely Newton’s second law; the motion equation for an arbitrary particle i is given as

$$m_i\ddot{x}_i = F_i^{ext} - F_i^{int} - F_i^{dmp} \quad (1)$$

where m_i, $\ddot{x}_i$, F_i^{ext}, F_i^{int}, F_i^{dmp} are the mass, acceleration vector, externalforce vector, internal force vector and damping force vector of particle i, respectively. F_i^{ext} consists of the concentrated force vector $[f_{ix}\ f_{iy'}]^T$ and equivalent force vector (from body force or surface force) $[f_{jx}^{ext}\ f_{jy}^{ext}]^T$ of element j on particle i, the internal force vector $F_i^{int} = [f_{ix}^{int}\ f_{iy}^{int}]^T$, and the damping force vector $F_i^{dmp} = [f_{ix}^{dmp}\ f_{iy}^{dmp}]^T$.

2.2 Particle internal force calculation

To calculate the internal forces, pure deformation of the element is essential. Fictitious reverse motion is adopted to obtain the pure deformation by deducting the displacement caused by the rigid body translation and rotation from the total displacement.

As shown in Fig.1, the planar element geometry is defined by three particles with node numbers (1, 2, 3) at time t and (1_a, 2_a, 3_a) at time ta. The position vectors of node j (j = 1, 2, 3) at ta and t are ja x and x_j, respectively. From t_a to t, the increments of node translations are

$$u^j = x^j - x_a^j \quad (2)$$

The triangular element at time t has undergone a rigid body motion, including rigid body translation and rigid body rotation. It is assumed that the displacement increments of node 1 are the rigid body translation of the element. For deducting the displacement caused by rigid body translation, a fictitious reverse rigid translation ($-u_1$) of the triangular element is applied from t to t_a, as shown in Fig.1, and the relative displacements are

$$\eta^j = u^j + (-u^1),\ j=1,2,3 \quad (3)$$

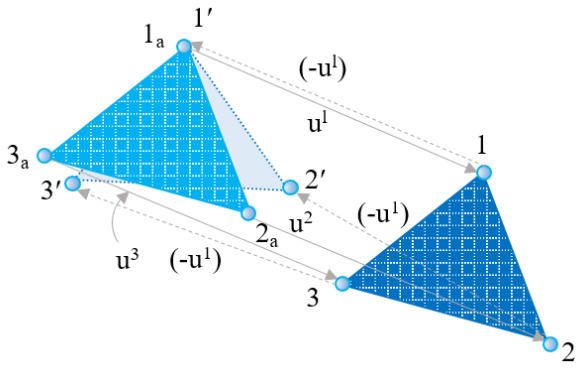

Figure 1: Reverse motion of element with three particles

Then the fictitious reverse rigid body rotation (-θ) is adopted to deduct the displacement caused by rigid body rotation, as shown in Fig. 2, and the nodal displacements due to the in-plane rigid body rotation displacement are

$$\eta_r = [R_r(-\theta) - I](x - x^1) \quad (4)$$

where $R_r(-\theta) = \begin{bmatrix} \cos(-\theta) & \sin(-\theta) \\ -\sin(-\theta) & \cos(-\theta) \end{bmatrix}$ is the rotation matrix.

Pure deformation of the nodes, η_d^j, can be expressed as

$$\eta_d^j = \eta^j + \eta_r^j \quad (5)$$

By taking the deformation vector of particle 2 as the basis vector, the direction vector of new coordinates e_1 and e_2 can be expressed as

$$e_1 = \frac{\eta_d^j}{|\eta_d^j|} = \begin{bmatrix} l \\ m \end{bmatrix} \text{ and } e_2 = \begin{bmatrix} -m \\ l \end{bmatrix} \quad (6)$$

Then, the pure deformation vector at the deformation coordinate can be written as

$$\Delta u_i = Q \Delta \eta_i^d \quad (i=1,2,3) \quad (7)$$

where $Q = \begin{bmatrix} l & m \\ -m & l \end{bmatrix}$ is the transform matrix of the deformation coordinates. Corresponding strain incrementation $\Delta\varepsilon$ and stress incrementation $\Delta\sigma$ can be calculated on the basis of the selected displacement mode as follows:

$$\Delta\varepsilon = B \Delta u_i \quad (8)$$

$$\Delta\sigma = D\Delta\varepsilon \tag{9}$$

where B is the strain matrix and D is the elastic matrix.When Eq.(9) is considered and D is constant, the linearly elastic material is simulated, which stress is linear to the pure deformation. For different constitutive models, such as hyper-elastic material, stress may not be linear to pure deformation, which different strain measure should be considered.

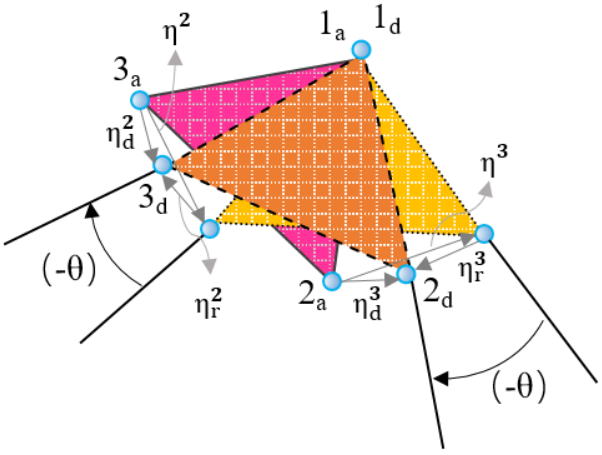

Figure 2: Fictitious reverse rigid-body rotation of a triangular element.

To further obtain nodal force incrementation Δf , the virtual research principle is adopted:

$$\delta W_e = (\delta\hat{u}^*)^T \hat{f} = (\delta\hat{u}^*)^T (\hat{f}_a + \Delta\hat{f}) \tag{10}$$

$$\hat{f}_a = t_a \int_S \hat{B}^T \hat{\sigma}_a dA \cong [\widehat{f_{2x}}\ \widehat{f_{3y}}\ \widehat{f_{3y}}]^T \tag{11}$$

$$\Delta\hat{f} = [\Delta\widehat{f_{2x}}\ \Delta\widehat{f_{3y}}\ \Delta\widehat{f_{3y}}]^T = (t_a \int_S \hat{B}^T D\hat{B} dA)\hat{u}^* \tag{12}$$

Following the force equilibrium of the current solid element, the rest of the unknown incrementation of the force components can be calculated as:

$$\sum \widehat{M_Z} = 0,\ \widehat{f_{2y}} = (-\widehat{f_{2x}}\hat{y}_2 + \widehat{f_{3x}}\hat{y}_3 - \widehat{f_{3y}}\hat{x}_3)/\hat{x}_2$$

$$\sum \widehat{F_x} = 0,\ \widehat{f_{1x}} = (-\widehat{f_{2x}} + \widehat{f_{3x}})$$

$$\sum \widehat{F_y} = 0,\ \widehat{f_{1y}} = (-\widehat{f_{2y}} + \widehat{f_{3y}}) \tag{13}$$

In order to calculate the sum of the equivalent nodal forces of all solid elements connected to the same mass at moment t. Thus, the force vector must transform to global coordinates for summation and time-integration as:

$$f_i = [\widehat{f_{ix}}\ \widehat{f_{iy}}]^T = \widehat{Q^T}\hat{f}_i \quad (i=1,2,3) \tag{14}$$

Then let the solid element return to position after undergoing translation (+u_1) and rotation (+θ) angle from experiencing the virtual position, so as to obtain the equivalent nodal force under the configuration at the current moment as, where R is the defined rotation matrix [5].

$$f_i = [f_{ix}\ f_{iy}]^T = Rf_i' \ (i=1,2,3) \tag{15}$$

After obtaining the internal force, the new particle position can be obtained from Eq. (1) using a center difference method. The trajectory of all particles can be solved following the sequence: start at the new position and calculate the new internal force to get the next new position.

3 DESCRIPTION OF CRACK PROPAGATION OF FPM AND COCM

There are many developed techniques for crack evaluation in concrete structures, including quarter point displacement, J-integral, FCM, two parameter fracture models, COCM.

This section introduces the FPM-COCM, combining FPM and COCM, to simluate crack propagation.

3.1 Description of crack in FPM

In FPM, a discretized particle model is adopted, in which solid fracture can be simulated by particle separation. Suppose the initial crack occurs as depicted in Fig. 3.

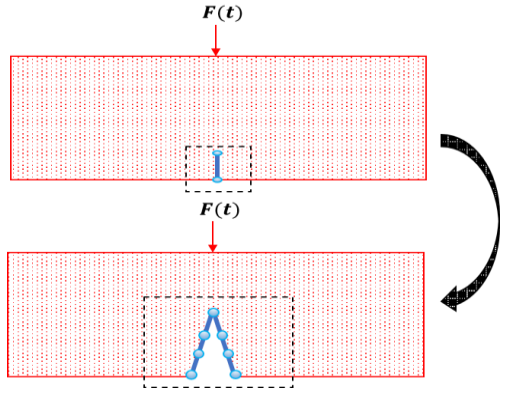

Figure 3: Fracture simulated by particle separation.

In crack propagation, primary particles separate into two new particles, and a new fracture surface is produced. In this study, solid fracture is assigned occur on the weak layer. Because the solid is attached to the fixed ground with the weak layer, the maximum tensile stress criterion is adopted as the fracture criterion:

$$\sigma_1 \leq [\sigma] \tag{16}$$

When certain fracture behavior occurs, corresponding external force, namely fracture force F^{frac}, should be considered on new separated particles, in which different crack propagation mechanisms can be taken into account. Thus Eq. (1) should be rewritten as Eq. (17).

Although FPM's implementation in fracture is relatively simple[6], the advantages can be demonstrated by simulating the fracture in combination with FPM and COCM later on.

$$m_i \ddot{x}_i = F_i^{ext} - F_i^{int} - F_i^{dmp} - F_i^{frac} \tag{17}$$

3.2 FPM-COCM method

The Cohesive Crack Model has been widely applied to simulate the damage process zone ahead of the crack tip in concrete structures [7-9] .

According to this model, the material behaves elastically during the first loading stage in Fig.4(a), whereas in the zone where the principal stress reaches the tensile strength, σ_t, the process zone starts developing. Within this zone, a cohesive law in Fig.4(b).

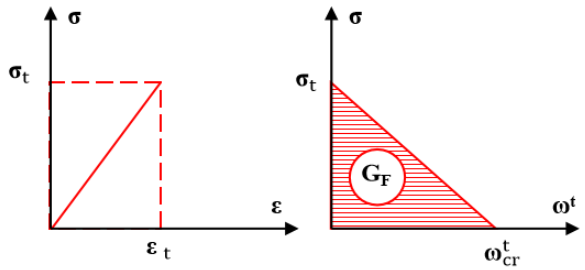

Figure 4: COCM: (a) pre-peak linear-elastico σ-ε law; (b) post-peak σ-ωt cohesive relationship

In the form σ-w^t, σ being the applied stress and w^t the crack opening, is adopted. Stresses apply until. the critical value of crack opening, wtcr, is reached: beyond this limit, the crack faces assume a stress-free condition.

In the present study, a cohesive constitutive law as:

$$\sigma = \sigma_t \left(1 - \frac{w^t}{w_{cr}^t}\right) \tag{18}$$

3.3 Numerical example

The numerically simulation using the FPM program with COCM to simulate the three-point bending test with a specimen geometry of l × d × b = 500 mm × 100 mm × 40 mm and a prefabricated crack of 30 mm in Fig. 5.

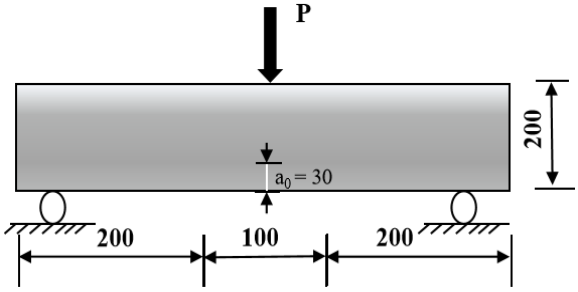

Figure 5: Schematic diagram of the specimen(mm)

Fig. 6 illustrates the stress distribution within the model, as computed by the fracture simulation program. Several critical time points were selected to systematically analyze the fracture progression:

Initially, in the absence of external force, the model exhibits neither stress nor deformation. As displacement loading intensifies, minor deformation becomes apparent, accompanied by stress concentration

at the tip of the pre-existing notch. With further displacement increase, the maximum tensile stress at the notch tip reaches the material's tensile strength, while additional stress concentrations emerge at both the loading point and support regions. The fracture process advances as the first node at the crack tip disconnects, causing the stress concentration to propagate forward. Ultimately, complete fracture occurs throughout the model, triggering the program's loop termination.

The simulated fracture process demonstrates excellent agreement with actual fracture behavior, providing further evidence that the FPM fracture program integrated with COCM effectively captures the fracture mechanics of solid materials.

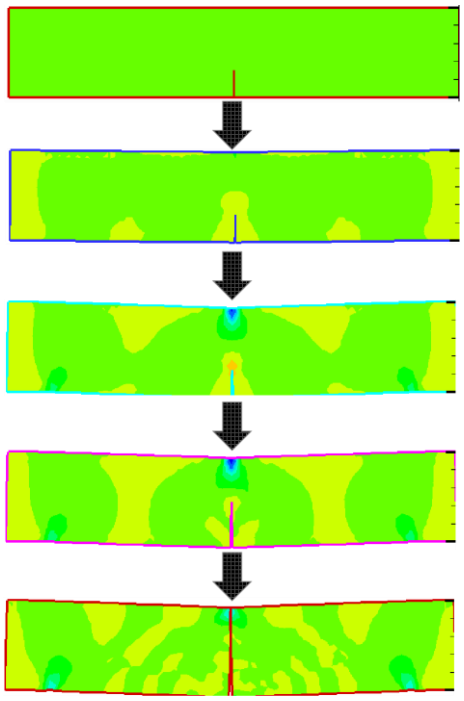

Figure 6: Stress contour of fracture process

4 CONCLUSIONS

This study introduces an innovative computational approach, the FPM-COCM method, for simulating crack propagation processes. The current research has successfully implemented the cohesive cracking simulation module within this framework.

Future work will focus on enhancing the FPM-COCM methodology by integrating the fictitious crack model into the FPM framework, thereby developing an efficient and robust solution for cohesive/overlapping crack propagation problems. The model's validity will be systematically evaluated through an extensive experimental program involving four-point bending tests on 54 pre-notched reinforced concrete (RC) beams. These tests will demonstrate the model's capability to accurately capture size-scale effects and failure mode transitions. Comprehensive analysis of key fracture characteristics, including load-bearing capacity, crack propagation patterns, and brittleness number, will further validate the model's effectiveness in representing the complex fracture behavior of concrete structures.

REFERENCES

[1] Belytschko, T., Fish, J. and Engelmann, B. E., 1995. A Finite Element with Embedded Localization Zones, *Computer Methods in Applied Mechanics and Engineering*, **70**: 59-89.

[2] Miehe, C. and Gürses, E., A Robust ,2007. Algorithm or Configurational - Force - Driven Brittle Crack Propagation with R-Adaptive Mesh Alignment, *International Journal for Numerical Methods in Engineering*, **72**: 127-155 .

[3] Belytschko, T. and Tabbara, M., 1996. Dynamic Fracture Using Element-Free Galerkin Methods, *International Journal for Numerical Methods in Engineering*, **39**: 923-938.

[4] Accornero F, Cafarelli R, Carpinteri A., 2021. The cohesive/overlapping crack model for plain and RC beams: Scale effects on cracking and crushing failures. *Magazine of Concrete Research*;**74**:433-450.

[5] Liu, F., Yu, Y., Wang, Q., Luo, Y, 2020. A coupled smoothed particle hydrodynamic and finite particle method: an efficient approach for fluid-solid

interaction problems involving free-surface flow and solid failure. *Eng. Anal. Bound. Elem*., **118**: 143–155.

[6] Carpinteri A, 1985. Interpretation of the Griffith instability as a bifurcation of the global equilibrium. *NATO ASI Series E: Appl Sci*. **94**:287–316.

[7] Carpinteri A, 1989. Cusp catastrophe interpretation of fracture instability. *J Mech Phys Solids*. **37(5)**:567–582.

[8] Carpinteri A, 1989. Size effects on strength, toughness, and ductility. *J Eng Mech (ASCE)*. **115(7)**:1375–1392.

[9] Hawkins NM, Hjorteset K, 1992. Minimum reinforcement requirements for concrete flexural elements. In: Carpinteri A, editor. *Application of Fracture Mechanics to Reinforced Concrete. London, UK: Elsevie*r. pp. 379–412.

[10] Carpinteri A, Corrado M, Mancini G, Paggi M, 2009. The overlapping crack model for uniaxial and eccentric concrete compression tests. *Mag Concr Res*. 61(9):745–757.